

# PULSE-SHAPING OFDM/BFDM SYSTEMS FOR TIME-VARYING CHANNELS: ISI/ICI ANALYSIS, OPTIMAL PULSE DESIGN, AND EFFICIENT IMPLEMENTATION

Dieter Schafhuber, Gerald Matz, and Franz Hlawatsch

Institute of Communications and Radio-Frequency Engineering, Vienna University of Technology  
Gusshausstrasse 25/389, A-1040 Vienna, Austria  
phone: +43 1 58801 38973, fax: +43 1 58801 38999, email: Dieter.Schafhuber@ieee.org  
web: <http://www.nt.tuwien.ac.at/dspgroup/time.html>

## ABSTRACT

This paper considers practically relevant aspects and advantages of *pulse-shaping* orthogonal/biorthogonal frequency division multiplexing (OFDM/BFDM) systems. We analyze the intersymbol/intercarrier interference (ISI/ICI) in such systems when they operate over time-varying channels. Two methods for an ISI/ICI-minimizing pulse design are proposed, and efficient FFT-based modulator and demodulator implementations are presented. Simulations show that for fast time-varying channels, optimized BFDM systems can outperform conventional OFDM systems with respect to ISI/ICI.

## 1. INTRODUCTION

**Background.** Orthogonal frequency division multiplexing (OFDM) is an attractive modulation scheme for high data-rate wireless communications [1–3]. Conventional OFDM, which employs rectangular transmit/receive pulses and a cyclic prefix (CP-OFDM) [2], is part of the standards IEEE 802.11a, Hiperlan/2, DAB-T, and DVB-T and is being considered for broadband wireless access by the IEEE 802.16 standardization work group. OFDM is also a promising candidate for future cellular communication systems.

*Pulse-shaping* OFDM systems and *biorthogonal frequency division multiplexing* (BFDM) systems [4–8] have several potential advantages over traditional CP-OFDM systems: higher bandwidth efficiency [4]; reduced sensitivity to carrier frequency offsets [5], oscillator phase noise, and narrow-band interference; and reduced intersymbol/intercarrier interference (ISI/ICI) [4]. Less ISI/ICI will be important for future communication systems where Doppler frequencies will be larger (equivalently, channel variations will be faster) due to higher carrier frequencies and/or higher mobile velocities. On the other hand, a potential drawback of BFDM systems relative to OFDM systems is noise enhancement [4].

The design of “optimal” OFDM/BFDM transmit and receive pulses is a current research topic [4, 6–8]. However, to the authors’ knowledge, performance results have been reported only for pulse-shaping OFDM/BFDM systems with spectral efficiencies  $\leq 0.5$ . In contrast, practical CP-OFDM systems have spectral efficiencies  $\geq 0.8$ . Also, it appears that no performance comparison of pulse-shaping OFDM/BFDM systems and CP-OFDM systems has been presented so far.

**Contributions and Organization.** Following a presentation of the system model in Section 2, Section 3 provides both an exact analysis of as well as approximations and bounds for the ISI/ICI power in pulse-shaping OFDM/BFDM systems operating over time-varying channels. In Section 4, we present two methods for an optimal pulse design based on a minimization of the ISI/ICI power. Section 5 proposes efficient, FFT-based modulator and demodulator implementations whose complexity is only slightly larger than for CP-OFDM systems. Finally, simulation results are presented in Section 6. It is shown that for practically relevant spectral efficiencies, the ISI/ICI power of optimized BFDM systems can be smaller than that of CP-OFDM systems by about 3 dB.

## 2. SYSTEM MODEL

**Modulator.** We consider a pulse-shaping OFDM/BFDM system with  $K$  subcarriers, symbol duration  $T$ , and subcarrier frequency spacing  $F$ . Time-frequency translates  $g_{l,k}(t) \triangleq g(t-lT)e^{j2\pi kF(t-lT)}$  of a transmit pulse  $g(t)$  are used to form the equivalent baseband transmit signal

$$s(t) = \sum_{l=-\infty}^{\infty} \sum_{k=0}^{K-1} a_{l,k} g_{l,k}(t). \quad (1)$$

Here,  $a_{l,k}$  ( $l \in \mathbb{Z}$ ,  $k \in \{0, \dots, K-1\}$ ) denotes the data symbol at symbol time  $l$  and subcarrier  $k$ . The symbols  $a_{l,k}$  are assumed i.i.d. with zero mean and mean power  $E\{|a_{l,k}|^2\} = \sigma_a^2$ .

**Channel.** Transmitting  $s(t)$  over a random time-varying channel  $\mathbb{H}$  with time-varying impulse response  $h(t, \tau)$  [9, 10] yields the received signal (integrals are from  $-\infty$  to  $\infty$ )

$$r(t) = (\mathbb{H}s)(t) = \int_{\tau} h(t, \tau) s(t-\tau) d\tau.$$

(In this paper, we will consider only the noiseless case.) The channel  $\mathbb{H}$  is assumed to satisfy the *wide-sense stationary uncorrelated scattering* (WSSUS) property. Thus, the second-order statistics of  $\mathbb{H}$  are described by the *Doppler spectrum* or *scattering function* [9]  $C_{\mathbb{H}}(\tau, \nu)$ , where  $\tau$  denotes time delay and  $\nu$  denotes Doppler frequency. Practical wireless WSSUS channels are *underspread* [4, 10, 11], i.e., their scattering function is effectively supported within a rectangular region  $\mathcal{S} \triangleq [0, \tau_{\max}] \times [-\nu_{\max}, \nu_{\max}]$  of area  $2\tau_{\max}\nu_{\max} \ll 1$ .

**Demodulator.** At the receiver, the demodulator computes the inner products of  $r(t)$  with time-frequency translates  $\gamma_{l,k}(t) \triangleq$

$\gamma(t-IT) e^{j2\pi kF(t-IT)}$  of a receive pulse  $\gamma(t)$ , i.e.,

$$x_{l,k} \triangleq \langle r, \gamma_{l,k} \rangle = \int_t r(t) \gamma_{l,k}^*(t) dt. \quad (2)$$

For pulse-shaping OFDM, there is simply  $\gamma(t) = g(t)$ . Perfect demodulation ( $x_{l,k} = a_{l,k}$  in the case of an ideal channel, i.e., for  $r(t) = s(t)$ ) is obtained if and only if the transmit/receive pulses satisfy the *biorthogonality condition*

$$\langle g, \gamma_{l,k} \rangle = \delta_l \delta_k. \quad (3)$$

For pulse-shaping OFDM, (3) reduces to the orthogonality condition  $\langle g, g_{l,k} \rangle = \delta_l \delta_k$ . A necessary condition for (3) to hold is  $TF \geq 1$ . However, because the spectral efficiency is proportional to  $1/(TF)$ , typically  $TF$  is chosen only slightly larger than 1. In particular, practical CP-OFDM systems are designed with  $TF$  ranging from 1.03 to 1.25, corresponding to a spectral efficiency of  $1/(TF) = 0.8 \dots 0.97$ . Whereas a larger  $TF$  results in a smaller spectral efficiency, it increases the freedom in designing pulses satisfying (3).

### 3. ISI/ICI ANALYSIS

**Exact Analysis.** In a pulse-shaping OFDM/BFDM system, the transmit symbols  $a_{l,k}$  and the received symbols  $x_{l,k}$  in (2) are related as [4]

$$x_{l,k} = \sum_{l'=-\infty}^{\infty} \sum_{k'=0}^{K-1} \langle \mathbb{H} g_{l',k'}, \gamma_{l,k} \rangle a_{l',k'}. \quad (4)$$

The terms in this sum with  $l' \neq l$  and/or  $k' \neq k$  describe the ISI and ICI introduced by the channel  $\mathbb{H}$ . A major advantage of OFDM/BFDM systems is that they allow simple scalar equalization. This is based on the approximation

$$x_{l,k} \approx H_{l,k} a_{l,k}, \quad \text{with } H_{l,k} \triangleq \langle \mathbb{H} g_{l,k}, \gamma_{l,k} \rangle,$$

which corresponds to neglecting the ISI/ICI terms in (4).

In what follows, we will consider the mean-square error introduced by this approximation or, equivalently, the *mean ISI/ICI power*

$$\sigma_{\Gamma}^2 \triangleq \mathbb{E}\{|x_{l,k} - H_{l,k} a_{l,k}|^2\}.$$

Using the statistical independence of the symbols  $a_{l,k}$ , one obtains  $\sigma_{\Gamma}^2 = \sigma_x^2 - \sigma_D^2$ , where  $\sigma_x^2 \triangleq \mathbb{E}\{|x_{l,k}|^2\}$  is the total received power and  $\sigma_D^2 \triangleq \mathbb{E}\{|H_{l,k} a_{l,k}|^2\}$  is the “desired” signal power. Using the WSSUS assumption, one can show that

$$\sigma_D^2 = \sigma_a^2 \int_{\tau} \int_{\nu} C_{\mathbb{H}}(\tau, \nu) |A_{\gamma,g}(\tau, \nu)|^2 d\tau d\nu, \quad (5)$$

with  $A_{\gamma,g}(\tau, \nu) \triangleq \int_t \gamma(t) g^*(t-\tau) e^{-j2\pi\nu t} dt$  denoting the cross-ambiguity function [12] of  $\gamma(t)$  and  $g(t)$ . Similarly, assuming an infinite number of subcarriers<sup>1</sup> ( $k \in \mathbb{Z}$ ), one can show

$$\sigma_x^2 = \sigma_a^2 \int_{\tau} \int_{\nu} C_{\mathbb{H}}(\tau, \nu) \mathcal{A}_{\gamma,g}(\tau, \nu) d\tau d\nu,$$

where  $\mathcal{A}_{\gamma,g}(\tau, \nu)$  is a periodized version of  $|A_{\gamma,g}(\tau, \nu)|^2$ , i.e.,

$$\mathcal{A}_{\gamma,g}(\tau, \nu) \triangleq \sum_{l=-\infty}^{\infty} \sum_{k=-\infty}^{\infty} |A_{\gamma,g}(\tau-IT, \nu-kF)|^2.$$

<sup>1</sup>This simplifying assumption results in an upper bound on the ISI/ICI power  $\sigma_{\Gamma}^2$  obtained for finite  $K$ . This bound is quite tight for large  $K$ .

Hence, the ISI/ICI power  $\sigma_{\Gamma}^2 = \sigma_x^2 - \sigma_D^2$  can be expressed as

$$\sigma_{\Gamma}^2 = \sigma_a^2 \int_{\tau} \int_{\nu} C_{\mathbb{H}}(\tau, \nu) [\mathcal{A}_{\gamma,g}(\tau, \nu) - |A_{\gamma,g}(\tau, \nu)|^2] d\tau d\nu. \quad (6)$$

It follows that  $\sigma_{\Gamma}^2$  will be small if  $\mathcal{A}_{\gamma,g}(\tau, \nu) - |A_{\gamma,g}(\tau, \nu)|^2$  is small within the effective support region  $\mathcal{S} = [0, \tau_{\max}] \times [-\nu_{\max}, \nu_{\max}]$  of  $C_{\mathbb{H}}(\tau, \nu)$ . This, in turn, requires that  $|A_{\gamma,g}(\tau-IT, \nu-kF)|^2$  for  $(l, k) \neq (0, 0)$  is small within  $\mathcal{S}$ . Equivalently,  $|A_{\gamma,g}(\tau, \nu)|^2$  has to be small within the regions  $\mathcal{S}_{l,k} \triangleq [lT, lT + \tau_{\max}] \times [kF - \nu_{\max}, kF + \nu_{\max}]$  with  $(l, k) \neq (0, 0)$ . We note that the biorthogonality relation (3) implies  $A_{\gamma,g}(IT, kF) = 0$  for  $(l, k) \neq (0, 0)$  and thus forces  $|A_{\gamma,g}(\tau, \nu)|^2$  to be zero at the center of  $\mathcal{S}_{l,k}$ .

**Approximations and Bounds.** The channel’s scattering function  $C_{\mathbb{H}}(\tau, \nu)$  is often not known exactly. Thus, an approximate expression of  $\sigma_{\Gamma}^2$  in terms of more global and more readily available channel parameters is desirable.

Because the channel is underspread,  $C_{\mathbb{H}}(\tau, \nu)$ —and, thus, the integrand in (6)—is well concentrated about the origin. We can here approximate  $|A_{\gamma,g}(\tau, \nu)|^2$  by the second-order Taylor series

$$|A_{\gamma,g}(\tau, \nu)|^2 \approx \sum_{n=0}^2 \frac{1}{n!} \left( \tau \frac{\partial}{\partial \tau} + \nu \frac{\partial}{\partial \nu} \right)^n |A_{\gamma,g}(\tau, \nu)|^2 \Big|_{(\tau, \nu)=(0,0)}.$$

Assuming real-valued and even-symmetric pulses that satisfy  $\int_t t \gamma(t) g(t) dt = 0$ ,  $\int_f f \Gamma(f) G(f) df = 0$ , and  $\langle g, \gamma \rangle = 1$ , this yields

$$|A_{\gamma,g}(\tau, \nu)|^2 \approx 1 - 4\pi^2 (B_{g,\gamma} \tau^2 + D_{g,\gamma} \nu^2), \quad (7)$$

where

$$D_{g,\gamma} \triangleq \int_t t^2 g(t) \gamma(t) dt, \quad B_{g,\gamma} \triangleq \int_f f^2 G(f) \Gamma(f) df$$

are measures of the “joint” duration and bandwidth, respectively, of the transmit pulse  $g(t)$  and the receive pulse  $\gamma(t)$ . Inserting (7) into (6) yields the approximation

$$\sigma_{\Gamma}^2 \approx \sigma_a^2 (\beta_1 + \beta_2), \quad (8)$$

with

$$\beta_1 \triangleq 4\pi^2 \sigma_{\mathbb{H}}^2 (\sigma_{\tau}^2 B_{g,\gamma} + \sigma_{\nu}^2 D_{g,\gamma}),$$

$$\beta_2 \triangleq \int_{\tau} \int_{\nu} C_{\mathbb{H}}(\tau, \nu) [\mathcal{A}_{\gamma,g}(\tau, \nu) - 1] d\tau d\nu.$$

Here,  $\sigma_{\mathbb{H}}^2 \triangleq \int_{\tau} \int_{\nu} C_{\mathbb{H}}(\tau, \nu) d\tau d\nu$  denotes the channel’s path loss, and

$$\sigma_{\tau}^2 \triangleq \frac{1}{\sigma_{\mathbb{H}}^2} \int_{\tau} \int_{\nu} \tau^2 C_{\mathbb{H}}(\tau, \nu) d\tau d\nu,$$

$$\sigma_{\nu}^2 \triangleq \frac{1}{\sigma_{\mathbb{H}}^2} \int_{\tau} \int_{\nu} \nu^2 C_{\mathbb{H}}(\tau, \nu) d\tau d\nu$$

are the channel’s delay spread and Doppler spread, respectively. For  $\sigma_{\mathbb{H}}^2$ ,  $\sigma_{\tau}^2$  and  $\sigma_{\nu}^2$  given,  $\beta_1$  can be interpreted as a measure of the “joint” time-frequency concentration of  $g(t)$  and  $\gamma(t)$ . Furthermore,  $\beta_2$  can be interpreted as a measure of how strongly the pulses  $g(t)$  and  $\gamma(t)$  deviate from those of an OFDM system. Indeed, for (pulse-shaping) OFDM satisfying

the orthogonality condition  $\langle g, g_{l,k} \rangle = \delta_l \delta_k$ ,  $\mathcal{A}_{g,g}(\tau, \nu) \equiv 1$  [13] and consequently  $\beta_2 = 0$ . We conclude that small ISI/ICI is achieved if  $g(t)$  and  $\gamma(t)$  are similar to OFDM pulses and well time-frequency localized.

If  $C_{\mathbb{H}}(\tau, \nu)$  is supported within  $\mathcal{S} = [0, \tau_{\max}] \times [-\nu_{\max}, \nu_{\max}]$ , one can derive the even simpler upper bounds

$$\beta_1 \leq 4\pi^2 \sigma_{\mathbb{H}}^2 (\tau_{\max}^2 B_{g,\gamma} + \nu_{\max}^2 D_{g,\gamma}),$$

$$\beta_2 \leq \sigma_{\mathbb{H}}^2 \max_{(\tau, \nu) \in \mathcal{S}} |\mathcal{A}_{\gamma,g}(\tau, \nu) - 1|,$$

which depend only on the global channel parameters  $\tau_{\max}$ ,  $\nu_{\max}$ ,  $\sigma_{\mathbb{H}}^2$  and on the pulses  $g(t)$ ,  $\gamma(t)$ .

For a conventional CP-OFDM system with a cyclic-prefix length  $T_{\text{cp}}$  that is larger than the channel's maximum delay, (8) can be shown to simplify to  $\sigma_{\text{I}}^2 \approx \frac{\pi^2}{3} \sigma_{\mathbb{H}}^2 \sigma_{\nu}^2 (T - T_{\text{cp}})^2$ . This expression generalizes results obtained for Jakes and uniform Doppler spectra [14] and for "frequency offset" channels [15].

#### 4. OPTIMAL PULSE DESIGN

We now present two methods for designing the pulses  $g(t)$ ,  $\gamma(t)$  such that the ISI/ICI power  $\sigma_{\text{I}}^2$  is minimized. These methods are based on the following alternative expression of  $\sigma_{\text{I}}^2$  [4]:

$$\sigma_{\text{I}}^2 = \sigma_{\text{I}}^2(g, \gamma) = \sigma_a^2 \int_{\tau} \int_{\nu} \mathcal{C}_{\mathbb{H}}(\tau, \nu) |A_{\gamma,g}(\tau, \nu)|^2 d\tau d\nu, \quad (9)$$

with

$$\mathcal{C}_{\mathbb{H}}(\tau, \nu) \triangleq \sum_{l \neq 0} \sum_{k \neq 0} C_{\mathbb{H}}(\tau - lT, \nu - kF).$$

Note that  $\mathcal{C}_{\mathbb{H}}(\tau, \nu)$  is a periodized scattering function with the  $l = k = 0$  component  $C_{\mathbb{H}}(\tau, \nu)$  omitted. If the scattering function is not known, or if good pulses for a whole range of scattering functions are to be found, one may use a default  $C_{\mathbb{H}}(\tau, \nu)$  that is constant on  $\mathcal{S} = [0, \tau_{\max}] \times [-\nu_{\max}, \nu_{\max}]$  and zero outside  $\mathcal{S}$ . This merely requires specification of the maximum delay  $\tau_{\max}$  and the maximum Doppler  $\nu_{\max}$ .

**First Design Method.** Our first pulse design method presupposes a prescribed transmit pulse  $g^{(0)}(t)$ . The ISI/ICI power  $\sigma_{\text{I}}^2(g^{(0)}, \gamma)$  is minimized with respect to the receive pulse  $\gamma(t)$ , subject to the biorthogonality condition (3). This is possible because for a fixed  $g(t)$  and  $TF > 1$ ,  $\gamma(t)$  is not uniquely determined by (3). Using results from Weyl-Heisenberg frame theory [12], it can be shown that all receive pulses satisfying (3) for the given  $g^{(0)}(t)$  can be written as [12, p. 142]

$$\gamma(t) = \gamma^{(0)}(t) + \sum_i c_i u_i(t), \quad (10)$$

where  $\gamma^{(0)}(t)$  is the so-called "canonical dual" of  $g^{(0)}(t)$ ,  $\{u_i(t)\}$  is an orthonormal basis determined by  $g^{(0)}(t)$  (more precisely, an orthonormal basis of the orthogonal complement of the space spanned by  $\{g_{l,k}^{(0)}(t)\}$ ), and the  $c_i$  are arbitrary coefficients. Using (10), the constrained minimization of  $\sigma_{\text{I}}^2(g^{(0)}, \gamma)$  becomes equivalent to an *unconstrained* minimization with respect to the coefficients  $c_i$ . The ISI/ICI power  $\sigma_{\text{I}}^2(g^{(0)}, \gamma)$  is a quadratic functional of the  $c_i$ . It can thus be shown that this minimization amounts to solving the system

of linear equations<sup>2</sup>  $\mathbf{B}\mathbf{c} = -\mathbf{a}$ , where  $[c]_i = c_i$  and

$$[\mathbf{B}]_{i,j} = \int_{\tau} \int_{\nu} \mathcal{C}_{\mathbb{H}}(\tau, \nu) A_{u_i, g^{(0)}}^*(\tau, \nu) A_{u_j, g^{(0)}}(\tau, \nu) d\tau d\nu,$$

$$[\mathbf{a}]_i = \int_{\tau} \int_{\nu} \mathcal{C}_{\mathbb{H}}(\tau, \nu) A_{u_i, g^{(0)}}^*(\tau, \nu) A_{\gamma^{(0)}, g^{(0)}}(\tau, \nu) d\tau d\nu.$$

Hence, the optimal biorthogonal receive pulse is given by  $\gamma^{\text{opt}}(t) = \gamma^{(0)}(t) + \sum_i c_i^{\text{opt}} u_i(t)$ , where  $c_i^{\text{opt}} = [\mathbf{c}^{\text{opt}}]_i$  with  $\mathbf{c}^{\text{opt}} = -\mathbf{B}^{-1}\mathbf{a}$ . The same approach can be used to optimize the transmit pulse  $g(t)$  for a prescribed receive pulse  $\gamma^{(0)}(t)$ .

**Second Design Method.** To further reduce the ISI/ICI power, we next propose to minimize  $\sigma_{\text{I}}^2$  normalized by  $\sigma_{\text{D}}^2 = E\{|H_{l,k} a_{l,k}|^2\}$  with respect to *both*  $g(t)$  and  $\gamma(t)$  simultaneously. Thus, the cost function to be minimized is  $J(g, \gamma) \triangleq \sigma_{\text{I}}^2 / \sigma_{\text{D}}^2$ , with  $\sigma_{\text{I}}^2$  and  $\sigma_{\text{D}}^2$  given by (9) and (5), respectively. Note that  $J(g, \gamma)$  is the reciprocal of the signal-to-interference ratio (SIR)  $\sigma_{\text{D}}^2 / \sigma_{\text{I}}^2$ . The biorthogonality constraint is now dropped for the sake of increased pulse design freedom. Thus, the optimized pulses will not be exactly biorthogonal, which means that some ISI/ICI will occur even for an ideal channel. However, this is not a problem because an ideal channel never occurs in practice. Moreover, we observed that the optimized pulses tend to be almost biorthogonal.

Because  $J(g, \gamma)$  depends nonquadratically on  $g(t)$ ,  $\gamma(t)$ , we use the numerical minimization function *fminunc* from MATLAB's optimization toolbox. In general, the resulting "optimal" pulses merely correspond to a local minimum of  $J(g, \gamma)$  instead of the global minimum desired, and they depend on the pulses used for initializing the minimization.

Simulation results for both design methods will be presented in Section 6.

#### 5. EFFICIENT IMPLEMENTATION

We next propose an efficient digital implementation of the modulator and demodulator in a pulse-shaping OFDM/BFDM system. We assume that all signals are sampled at a rate that is equal to the system bandwidth  $KF$ . In the resulting discrete-time, normalized-frequency setting, the subcarrier spacing is  $1/K$  and the discrete symbol duration is  $N = KTF$ . The sampled transmit and receive pulses are assumed to have finite length which will be denoted by  $L_g$  and  $L_\gamma$ , respectively.

As shown in Fig. 1, the proposed implementations essentially consist of the usual length- $K$  IDFT or DFT that is also required in CP-OFDM systems, a pulse-shaping operation (elementwise multiplication by the vector  $\mathbf{g} = (g[0] \cdots g[L_g - 1])^T$  or  $\boldsymbol{\gamma} = (\gamma[0] \cdots \gamma[L_\gamma - 1])^T$ ), and an overlap/add or pre-aliasing operation. We note that in practically relevant scenarios where  $TF = N/K$  is only slightly larger than 1, polyphase implementations [16] are not possible since they would require  $TF$  to be an integer.

**Modulator.** The digital OFDM/BFDM modulator computes the transmit signal (cf. (1))

$$s[n] = \frac{1}{\sqrt{K}} \sum_{l=-\infty}^{\infty} \sum_{k=0}^{K-1} a_{l,k} g[n - lN] e^{j2\pi \frac{k}{K}(n - lN)}.$$

<sup>2</sup>In practical digital implementations, the matrix  $\mathbf{B}$  and the vectors  $\mathbf{a}$  and  $\mathbf{c}$  are finite-dimensional.

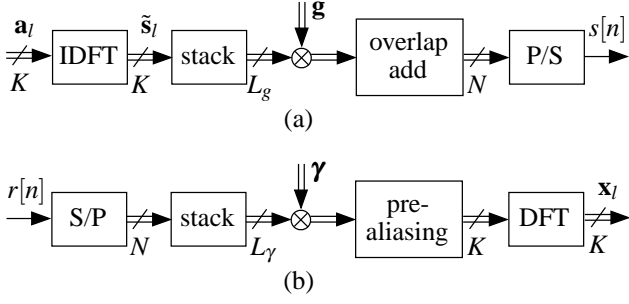


**Figure 1:** Efficient digital implementation of a pulse-shaping OFDM/BFDM system: (a) Modulator, (b) demodulator.

Within the  $l$ th symbol period,  $s[n]$  can be written as

$$s[n] = \sum_{i=l-Q_g}^{l+Q_g} s_i^{(g)}[n-iN], \quad n \in [lN, (l+1)N-1], \quad (11)$$

where  $Q_g = \lceil L_g/(2N) \rceil$  and

$$s_i^{(g)}[n] = \tilde{s}_i[n]g[n], \quad \text{with } \tilde{s}_i[n] = \frac{1}{\sqrt{K}} \sum_{k=0}^{K-1} a_{l,k} e^{j2\pi \frac{nk}{K}}. \quad (12)$$

Equation (11) describes an overlap/add operation that involves  $2Q_g + 1$  windowed IDFT signals  $s_i^{(g)}[n]$  (see (12)). These can be computed by periodically repeating (stacking) the vector  $\tilde{s}_i = (\tilde{s}_i[0] \dots \tilde{s}_i[K-1])^T$  containing the length- $K$  normalized IDFT of the  $a_{l,k}$  to form a length- $L_g$  vector. Subsequently, this vector is multiplied elementwise by the transmit pulse vector  $g$ . The resulting efficient implementation of the modulator is shown in Fig. 1(a).

**Demodulator.** At the receiver, demodulation of the received signal  $r[n]$  is performed according to (cf. (2))

$$x_{l,k} = \frac{1}{\sqrt{K}} \sum_{n=-\infty}^{\infty} r[n] \gamma^*[n-lN] e^{-j2\pi \frac{k}{K}(n-lN)}.$$

This can be efficiently implemented by means of the length- $K$  normalized DFT

$$x_{l,k} = \frac{1}{\sqrt{K}} \sum_{n=0}^{K-1} \tilde{r}_l^{(\gamma)}[n] e^{-j2\pi \frac{kn}{K}}.$$

Here, the length- $K$  sequence  $\tilde{r}_l^{(\gamma)}[n]$  is obtained from the windowed received signal  $r_l^{(\gamma)}[n] \triangleq r[n+lN]\gamma^*[n]$  via the ‘‘pre-aliasing’’ operation

$$\tilde{r}_l^{(\gamma)}[n] = \sum_{i=-Q_\gamma}^{Q_\gamma} r_l^{(\gamma)}[n+iK],$$

with  $Q_\gamma = \lceil L_\gamma/(2K) \rceil$ . This leads to the efficient demodulator implementation sketched in Fig. 1(b).

**Computational Complexity.** The complexity of the modulator is determined by the IDFT and the pulse shaping, requiring a total of  $\mathcal{O}(K \log_2 K + L_g)$  operations per symbol period. Similarly, the DFT and windowing at the receiver amount to  $\mathcal{O}(K \log_2 K + L_\gamma)$  operations per symbol period. Compared to a CP-OFDM system that requires only the IDFT/DFT (i.e.,

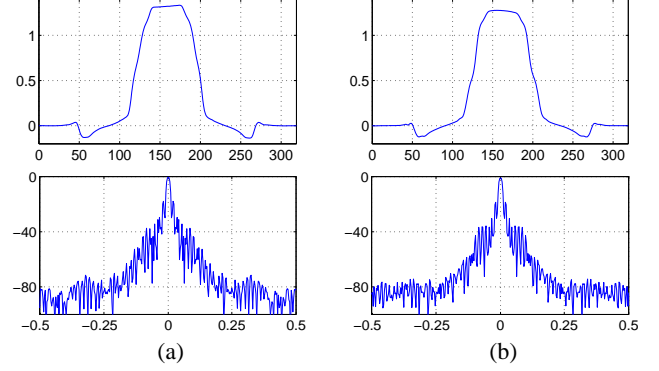


**Figure 2:** Pulse shape (top) and Fourier transform magnitude (bottom, in dB) of (a) the transmit pulse and (b) the receive pulse of the BFDM system  $\mathcal{G}_{II}$ .

no pulse-shaping), this is an increase by  $L_g + L_\gamma$  operations per symbol period. As an example, for a BFDM system with  $K = 1024$  carriers, symbol length  $N = 1280$ , and pulse length  $L_g = L_\gamma = 2N$ , the increase in computational complexity with respect to a CP-OFDM system is only 25%. We note that due to the overlap/add and pre-aliasing operations, pulse-shaping OFDM/BFDM systems require additional memory and introduce a latency of a few symbol periods.

## 6. SIMULATION RESULTS

**BFDM System Design.** We consider four BFDM systems and a reference CP-OFDM system with transmit bandwidth  $KF = 1$  MHz,  $K = 64$  subcarriers, symbol duration  $T = 80 \mu\text{s}$ , and subcarrier spacing  $F = 15.625$  kHz. We thus have  $TF = 1.25$ , which corresponds to a spectral efficiency parameter of  $1/(TF) = 0.8$ . Assuming a sampling frequency of 1 MHz, we obtain the discrete-time symbol duration as  $N = 80$ . The cyclic prefix of the CP-OFDM system has length  $16 \mu\text{s}$ . The pulse length of the BFDM systems is  $L = L_g = L_\gamma = 320$ . The scattering function used for the BFDM pulse design is constant on  $\mathcal{S} = [0, \tau_{\max}] \times [-v_{\max}, v_{\max}]$  with  $\tau_{\max} = 8 \mu\text{s}$  and  $v_{\max} = 625$  Hz and zero outside  $\mathcal{S}$ .

We designed two BFDM systems, denoted by  $\mathcal{G}_I$  and  $\mathcal{R}_I$ , by prescribing a (truncated) Gaussian transmit pulse and a rectangular transmit pulse, respectively and computing the optimal receive pulse using the first design method from Section 4. Two further BFDM systems  $\mathcal{G}_{II}$  and  $\mathcal{R}_{II}$  were designed using the second design method from Section 4. Here, the minimization procedure was initialized by a Gaussian transmit pulse ( $\mathcal{G}_{II}$ ) and a rectangular transmit pulse ( $\mathcal{R}_{II}$ ) and the associated canonical duals for the receive pulses.

For illustration, the transmit and receive pulses of  $\mathcal{G}_{II}$  are shown in Fig. 2. It is seen that both pulses consist of a main lobe of width  $\approx N$  and small sidelobes. The two pulses are very similar, which means that  $\mathcal{G}_{II}$  is almost an OFDM system (the angle between  $g[n]$  and  $\gamma[n]$  is about  $7.5^\circ$ , as compared to  $0^\circ$  for pulse-shaping OFDM). This is important because a BFDM system in which  $\gamma[n]$  is very different from  $g[n]$  may suffer from noise enhancement at the receiver [4].

**SIR Performance.** Fig. 3 shows the SIR  $\sigma_D^2/\sigma_I^2$  obtained with our BFDM systems and with the reference CP-OFDM

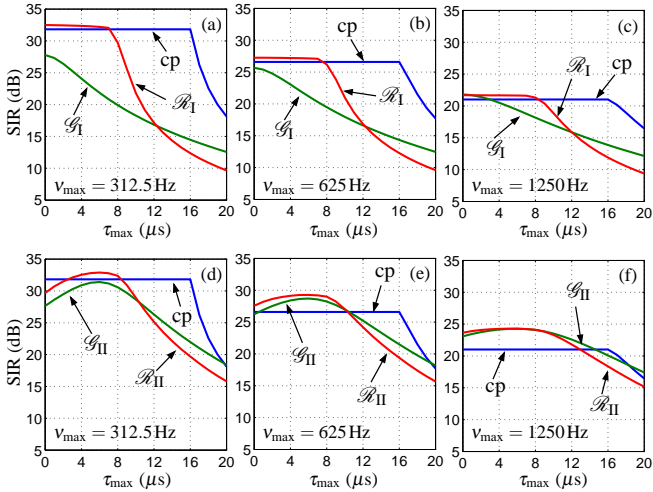


**Figure 3:** SIR obtained with the four BFDM systems  $\mathcal{G}_I$ ,  $\mathcal{R}_I$ ,  $\mathcal{G}_{II}$ , and  $\mathcal{R}_{II}$  and the CP-OFDM system (denoted “cp”): (a)–(c)  $\mathcal{G}_I$ ,  $\mathcal{R}_I$ , and cp; (d)–(f)  $\mathcal{G}_{II}$ ,  $\mathcal{R}_{II}$ , and cp.

system for different channel scattering functions. These scattering functions are constant on  $\mathcal{S} = [0, \tau_{\max}] \times [-v_{\max}, v_{\max}]$  and zero outside  $\mathcal{S}$ , with  $\tau_{\max}$  ranging from 0 to 20  $\mu\text{s}$  and  $v_{\max} \in \{312.5 \text{ Hz}, 625 \text{ Hz}, 1250 \text{ Hz}\}$ . Note that the scattering functions are generally different from those for which our pulses were designed (for pulse design, we used  $\tau_{\max} = 8 \mu\text{s}$  and  $v_{\max} = 625 \text{ Hz}$ ), thus assessing the robustness of our designs. It is seen that the SIR of  $\mathcal{G}_I$  is smaller than that of CP-OFDM for virtually all channel parameters, and the SIR of  $\mathcal{R}_I$  is just slightly larger than that of CP-OFDM for  $\tau_{\max} \leq 8 \mu\text{s}$  and all  $v_{\max}$ . On the other hand, the BFDM systems  $\mathcal{G}_{II}$  and  $\mathcal{R}_{II}$  achieve an SIR improvement of up to about 3 dB over the CP-OFDM system in certain ranges of  $\tau_{\max}$  and  $v_{\max}$ .

To further illustrate this potential SIR advantage of BFDM, Fig. 4 identifies the regions in the  $(\tau_{\max}, v_{\max})$ -plane where the best SIR performance is achieved by  $\mathcal{G}_{II}$  (light grey),  $\mathcal{R}_{II}$  (dark grey), and CP-OFDM (white). It is seen that the BFDM systems  $\mathcal{G}_{II}$  and  $\mathcal{R}_{II}$  outperform CP-OFDM for a wide range of channel parameters, especially for large Doppler frequencies, i.e., fast time-varying channels.

## 7. CONCLUSIONS

We presented an ISI/ICI-optimal design of the transmit and receive pulses of BFDM systems operating over time-varying channels. Using this design, we demonstrated that for realistic values of spectral efficiency and for fast time-varying channels (i.e., large Doppler), the SIR of BFDM systems can be larger than that of conventional CP-OFDM systems by about 3 dB. We also presented an ISI/ICI analysis of pulse-shaping OFDM/BFDM systems, as well as efficient FFT-based modulator and demodulator implementations that are only slightly more complex than those of CP-OFDM systems.

## ACKNOWLEDGMENT

The authors are grateful to K. Gröchenig and H. G. Feichtinger for stimulating discussions.

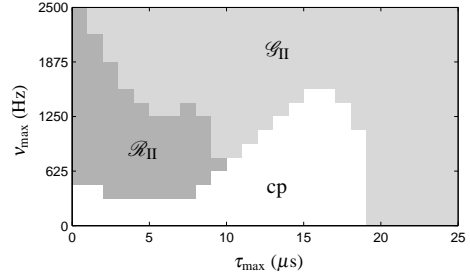


**Figure 4:** Regions in the  $(\tau_{\max}, v_{\max})$ -plane where  $\mathcal{G}_{II}$ ,  $\mathcal{R}_{II}$ , and CP-OFDM (cp) outperform the respective other systems.

## REFERENCES

- [1] R. W. Chang, “Synthesis of band-limited orthogonal signals for multi-channel data transmission,” *Bell Syst. Tech. J.*, vol. 45, pp. 1775–1796, Dec. 1966.
- [2] A. Peled and A. Ruiz, “Frequency domain data transmission using reduced computational complexity algorithms,” in *Proc. IEEE ICASSP-80*, (Denver, CO), pp. 964–967, 1980.
- [3] P. Smulders, “Exploiting the 60 GHz band for local wireless multimedia access: Prospects and future directions,” *IEEE Comm. Mag.*, pp. 140–147, Jan. 2002.
- [4] W. Kozek and A. F. Molisch, “Nonorthogonal pulseshapes for multicarrier communications in doubly dispersive channels,” *IEEE J. Sel. Areas Comm.*, vol. 16, pp. 1579–1589, Oct. 1998.
- [5] P. K. Remvik and N. Holte, “Carrier frequency offset robustness for OFDM systems with different pulse shaping filters,” in *Proc. IEEE GLOBECOM-97*, (Phoenix, AZ), pp. 11–15, 1997.
- [6] A. Vahlin and N. Holte, “Optimal finite duration pulses for OFDM,” *IEEE Trans. Comm.*, vol. 4, pp. 10–14, Jan. 1996.
- [7] R. Haas and J. C. Belfiore, “A time-frequency well-localized pulse for multiple carrier transmission,” *Wireless Personal Comm.*, vol. 5, pp. 1–18, 1997.
- [8] H. Bölcskei, “Efficient design of pulse shaping filters for OFDM systems,” in *Proc. SPIE Wavelet Applications in Signal and Image Processing VII*, (Denver, CO), pp. 625–636, July 1999.
- [9] P. A. Bello, “Characterization of randomly time-variant linear channels,” *IEEE Trans. Comm. Syst.*, vol. 11, pp. 360–393, 1963.
- [10] J. G. Proakis, *Digital Communications*. New York: McGraw-Hill, 3rd ed., 1995.
- [11] G. Matz and F. Hlawatsch, “Time-frequency characterization of random time-varying channels,” in *Time-Frequency Signal Analysis and Processing* (B. Boashash, ed.), Englewood Cliffs (NJ): Prentice Hall, 2002.
- [12] K. Gröchenig, *Foundations of Time-Frequency Analysis*. Boston: Birkhäuser, 2001.
- [13] R. Tolimieri and R. S. Orr, “Characterization of Weyl-Heisenberg frames via Poisson summation relationships,” in *Proc. IEEE ICASSP-92*, (San Francisco, CA), pp. 277–280, March 1992.
- [14] Y. Li and L. Cimini, “Bounds on the interchannel interference of OFDM in time-varying impairments,” *IEEE Trans. Comm.*, vol. 49, pp. 401–404, March 2001.
- [15] T. Pollet, M. V. Bladel, and M. Moeneclaey, “BER sensitivity of OFDM systems to carrier frequency offset and Wiener phase noise,” *IEEE Trans. Comm.*, vol. 43, pp. 191–193, Feb. 1995.
- [16] P. P. Vaidyanathan, *Multirate Systems and Filter Banks*. Englewood Cliffs (NJ): Prentice Hall, 1993.